Article:
Guo, F, He, Y, Hassanpour, A orcid.org/0000-0002-7756-1506 et al. (2 more authors) (2020) Thermogravimetric analysis on the co-combustion of biomass pellets with lignite and bituminous coal. Energy, 197. 117147. ISSN 0360-5442

https://doi.org/10.1016/j.energy.2020.117147

Thermogravimetric analysis on the co-combustion of biomass pellets with lignite and bituminous coal

Feihong Guo[1,2*], Yi He[2], Ali Hassanpour[2], Jabbar Gardy[2], Zhaoping Zhong[1*]

[1]Key Laboratory of Energy Thermal Conversion and Control of the Ministry of Education, School of Energy and Environment, Southeast University, Nanjing 210096, Jiangsu, China

[2]School of Chemical and Process Engineering, University of Leeds, Leeds, UK

ABSTRACT: This work presents comparative study on the combustion of biomass pellets (BP) with Bituminous coal (BC), and Xiao longtan lignite (XL) using thermogravimetric (TG) analysis. The results show that the combustion process of BP:BC can be divided into the release and combustion of volatile compounds, oxidation of BP char and combustion of BC char. Whilethere are two stages for the blend of XL and BP, which are the combustion of volatile compounds and the char burning of BP and XL. With increasing BP ratio, the maximum combustion rate and combustion index increase, while the burnout temperature decreases, indicating the combustion performance of coal can be improved. In addition, interactions between BP and XL are more significant than that of BP and BC. The maximum deviations are found to be 30% BP with BC and 10% BP with XL. Reaction mechanisms are analysed using Coats–Redfern method. The first order model is found to be suitable for the first stage of biomass burn (stage 1) and coal combustion of BC:BP blends. Diffusion controlled model D3 and D4 are the most effective for the second stage of biomass burn and XL combustion, respectively. The minimum activation energies of biomass blending is obtained with a BP ratio of 30% for BC and 10% for XL.

KEYWORDS: Biomass Pellets, bituminous coal, lignite, combustion, thermogravimetric analysis

1. Introduction

Biomass pellets (BP) are used in combustion engineering due to its higher density and combustion efficiency than that of biomass feedstock [1]. Wood fuel is the main source of raw material for the production of biomass pellets. The increasing need of biomass pellets results in a shortage of wood fuel. Therefore, mixing non-woody biomasses with wood fuel becomes an effective way to provide sustainable source materials for biomass pellets production, such as rice straw and catkins [2]. Rice straw

is a kind of agricultural residues with rich resources, which is widely used. Catkins are a type of compact or string-like inflorescence, produced from birches, willows, and oaks. They float easily in air, and excessive catkins often cause environmental pollution and disease transmission [3]. However, so far there is no effective method to dispose disposal catkins. Therefore, BP used in this study is a kind of innovative composite biomass pellets, including wood waste, rice straw, and catkins.

Compared to coal, biomass has the advantages of low sulfur, low nitrogen and stable combustion. Therefore, the co-combustion of coal and biomass may be an ideal method for biomass waste. Biomass possesses higher volatile matter, shorter combustion time and lower ignition temperature, which has significantly different characteristics as compared to coal [4]. Therefore, it is necessary to study the thermodynamic characteristics of coal-biomass co-combustion. Compared with other analytical methods, thermogravimetric analysis (TG) is more convenient, fast and efficient, which is widely used in the field of combustion [5]. There are numerous researches presenting thermogravimetric analyses of coal, biomass and their blends. **Table 1** is the short literature review of the co-combustion of different coal and biomass types.

Magalhães et al. [6] studied the combustion behavior and kinetics of lignite and olive residue. Tunçbilek and Soma lignite had one major combustion stage and olive residue had two distinct stages for combustion. Kinetic analysis using Coats–Redfern method showed that Tunçbilek lignite had the highest activation energy. In contrast, during the combustion of laying hens manure and coal [7], it was concluded that

activation energy was much higher for biomass than for coal. Moreover, the blended activation energy was increasing with increased biomass content. Jayaraman et al. [8] confirmed the activation energy of biomass was higher than that of coal because of the pore structures. Wang et al. [9] investigated the co-combustion of coal and the biomass (sawdust and rice straw). Kinetic calculation indicated the larger the biomass proportion, the lower the activation energy of blends. In addition, it was found that there was interaction between coal and biomass. Ignition and the burnout temperature were decreasing with increasing biomass ratio. As biomass ratio is 70%, the blends displayed the maximum burning rate and best combustion performance. By TG experiments, Ullah et al. [10] demonstrated that the ignition behavior and thermal reactivity of coal were improved by the addition of pine wood. Moreover, activation energy increased in volatiles burning profile and decreased in char combustion stage with elevated biomass proportion. Experiments by Wang et al. [11] showed that there was synergistic effect during combustion process of biomass and coal, the ignition performance was improved by increasing biomass. Activation energies had the lowest value at 60% rice husk (rice husk and coal), 20% pine sawdust (first stage of pine sawdust and coal), and 40% pine sawdust (second stage of pine sawdust and coal). Liu et al. [12] found that hydrochar addition increased the combustion efficiency of blends due to synergistic interactions between hydrochar and lignite. The first-order reaction mechanism can describe the combustion process of blends well. Li et al. [13] demonstrated that the addition of distillation residue can improve the combustion efficiency of lignite. With increasing distillation residue, the synergistic interactions between distillation residue and lignite

77 firstly increased and then decreased. Moreover, the optimum mixture ratio of
78 distillation residue (60%) in blends was obtained, with the lowest activation energy. Yu
79 et al. [14] confirmed the synergistic effect between lignite and eucalyptus bark during
80 their co-combustion and found 20-40% eucalyptus bark was the optimum blending ratio.
81 Coats–Redfern analysis presented that the combustion of eucalyptus bark and their
82 blends was controlled by diffusion model, and lignite burning was determined by
83 reaction order model.

84 However, because of the different species of biomass and coal, there are still
85 different or even contrary conclusions. Despina and Stelios [15] observed that there was
86 synergistic effect between lignite and cardoon, but there was no synergism between
87 lignite and pine needles. Toptas et al. [16] investigated the combustion behavior of
88 lignocellulosic and animal wastes, and their blends with lignite. The results indicated
89 that biomass addition can improve the burnout performance of lignite, and the blends
90 had a lower ignition and burnout temperature at 50% coal. However, there was no
91 interaction between the lignite and biomass at initial step of combustion. Gil et al. [17]
92 also demonstrated that there was no significant interaction between bituminous coal
93 and pine sawdust in co-combustion process, and the combustion steps in blends were
94 only the sum of the biomass and coal individual stages. In addition, Kawnish and
95 Sankar [18] performed pyrolysis experiments of algae–coal blends. The results
96 indicated that there was no interaction between the algae and coal during pyrolysis.

97 **Table 1** Thermogravimetric analysis of co-combustion: literature review

Fuel type	Method	Experimental conditions	Kinetic model	Ref.

Lignite from Tunçbilek and Soma, and olive residue	TG and FT-IR	Room temperature-1000 °C, 10 mg sample, 15, 20, 40 °C/min heating rate, and 120 ml/min flow air	Coats-Redfern	Magalhães et al. [6]
laying hens manure, coal, and blends	TG	Room temperature-1000 °C, 20 mg sample, 5, 10, 15, 20 °C/min heating rate, and 70 ml/min flow air	Ozawa-Flynn-Wall	Junga et al. [7]
Poplar wood, hazelnut shell, bituminous coal, and blends	TG-MS	Room temperature-950 °C, 10 mg sample, 20 °C/min heating rate, and 50 ml/min flow air	Arrhenius and Coats–Redfern	Jayaraman et al. [8]
Sawdust, rice straw, coal, and blends	TG	Room temperature-1273 K, 10 mg sample, 10 K/min heating rate, and 70 ml/min flow N_2 /air (10% air) mixture atmosphere	Coats-Redfern	Wang et al. [9]
Pine wood, coal , and blends	TG	Room temperature-800 °C, 10 mg sample, 20 °C/min heating rate, and 75 ml/min flow air	Coats–Redfern	Ullah et al. [10]
Bituminous coal, rice husk, pine sawdust, and blends	TG	Room temperature-900 K, 5 mg sample, 2.5, 5, 10, 20 K/min heating rate, and 100 ml/min flow air	Double parallel reactions *n*th order rate model	Wang et al. [11]
Hydrochar, lignite, and blends	TG	Room temperature-850 °C, 8 mg sample, 15 °C/min heating rate, and 20 ml/min flow air	Coats–Redfern	Liu et al. [12]
Pyrolysis oil distillation residue, lignite, and blends	TG	Room temperature-800 °C, 5 mg sample, 10, 20, 30, 40 °C/min heating rate, and 80 ml/min flow air	Coats–Redfern	Li et al. [13]
Eucalyptus bark, lignite, and blends	TG-MS	50-800 °C, 10 mg sample, 10, 15, 20 °C /min heating rate, and 100 ml/min flow air	Coats-Redfern	Yu et al. [14]
Olive prunnings, cotton residue, pine needles, cardoon, sewage sludge, lignite, and blends	TG	25-850°C, 20-25 mg sample, 3-100 °C/min heating rate, and 45 ml/min flow air	-	Despina and Stelios [15]
Lignocellulosic, animal wastes, and their blends with lignite	TG	Room temperature-900 °C, 30 mg sample, 20 °C/min heating rate, and 100 ml/min flow air	Coats–Redfern	Toptas et al. [16]

Bituminous coal, pine sawdust, and their blends	TG	Room temperature-1000 °C, 5 mg sample, 15 °C/min heating rate, and 50 cm^3/min flow air	Coats–Redfern	Gil et al. [17]

In general, the co-combustion of biomass with coal received fairly intensive studies. TG analysis can summarize combustion characteristics and kinetic model shows the variation of the activation energy. However, the reaction mechanisms between coal and biomass are not fully understood, and there are some different or even contrary conclusions [19]. In addition, there is nearly no research report regarding the utilization of catkins added into biomass pellets. In our study, the woody fuel is mixed with rice straw and catkins. It can not only provide source material, but also reduce the pollution emissions in the co-combustion process. Therefore, it is highly essential to fully understand the co-combustion processes of coal and mixed biomass pellets. The aim of this work is to determine the potential of mixed biomass pellets and to compare the co-combustion characteristics of different coal with mixed biomass pellets. Combustion characteristics and kinetic parameters are advantageous as a guide for the combustion application.

2. Experimental and methods

2.1 Materials

BP has a cylindrical shape with 5-10 mm in diameter and 5-20 mm in length, produced by Corn Stover Pellet Mill (ZLSP200B). Bituminous coal (BC) is the most popular coal with large yield, which is obtained from Huainan Coalfield in Anhui, China. Lignite acquired from Xiao longtan power plant (XL) in Yunnan is the lowest-grade coal with high contents of volatile matter and moisture. All samples are dried for

5 hours at 100 °C, then ground to powders and sieved to ensure that the particle size is smaller than 0.18 mm. The properties of BC, XL and BP are decipated in **Table 2**. BP is separately added to different coal (BC and XL) at weight ratios of 0:100, 10:90, 30:70, 50:50, 70:30, and 100:0. The contents of carbon and hydrogen are established by Liebig method (ISO 625:1996). The concentration of nitrogen is determined by Semi-micro Kjeldahl method (ISO 333:1996). The sulphur content is found by IR spectrometry (ISO 19579:2006). The remaining oxygen percentage is calculated by the difference. The proximate analysis is referred to GB/T 212-2008 standards. Element concentrations are analyzed by inductively coupled plasma-atomic emission spectrometry.

Table 2 Property of BC, XL and BP

Sample	Proximate analysis, (wt.%, ad. basis)				Ultimate analysis, (wt.%, daf. basis)					HV (kJ/kg)	Elemental analysis (g/kg)				
	Moisture	Ash	Volatile matter	Fixed carbon	C	H	N	S	O*		Ca	Fe	K	Na	S
BC	2.17	24.20	21.20	52.43	68.54	4.33	0.97	0.58	25.58	20.72	12.12	4.24	0.05	0.04	0.99
XL	9.16	36.50	28.81	25.53	39.59	3.63	0.79	1.67	45.68	15.68	32.62	6.56	0.59	0.08	16.17
BP	5.2	6.1	70.51	18.19	43.17	4.77	0.04	0.05	51.97	17.80	4.79	0.60	1.09	0.33	0.28

Notes: ad-air dry; daf-dry and free; HV-heating value; O*=1-(C+H+N+S).

2.2 Method

Thermogravimetric experiments are performed by TG 209 cell (Netzsch). The blending samples (10 mg) are heated from 25 to 900 °C under air atmosphere (80 ml/min) at heating rate of 20 °C/min. Both weight loss and temperature are obtained during the whole combustion. The combustion characteristic parameters are obtained from thermodynamic curves [3]. The value of differential thermogravimetric (DTG) is the slope for the TG corresponding to the point at the same temperature. This tangent intersects with dehydration smooth baseline and the temperature corresponding to the

intersection is defined as ignition temperature (T_i). The peak temperature and combustion rate corresponding to the first combustion stage are T_1 and DTG_1, respectively. The second, third, and average burning stages follow this rule, such as T_2, T_3, DTG_2, and DTG_3. At the zero value of DTG, the corresponding temperature is referred to the burnout temperature (T_b). The comprehensive combustion characteristic index (S) reflects the performance of material ignition and burnout, which is determined in **Eq.1.**

$$S = \frac{DTG_m DTG_a}{T_i^2 T_b} \quad (1)$$

where DTG_m is the maximum mass lose rate and DTG_a means the average mass loss rate, which is determined by total consumption of sample mass and reaction time.

2.3 Kinetic theory

Combustion is a complex process, including gas phase and solid-gas reactions[17]. Kinetics parameters can be obtained based on Arrhenius equation (Eq. 2).

$$\frac{da}{dt} = Ae^{\frac{-E}{RT}} f(a) \quad (2)$$

where a is the mass conversion ratio, t is time, A is pre-exponential factor, E is activation energy, R is gas constant, T is absolute temperature, and $f(a)$ is decided by reaction mechanism. When heating rate ($w=dT/dt$) is constant, Eq.2 is transformed into Eq.3.

$$g(a) = \int_0^a \frac{da}{f(a)} = \frac{A}{w}\int_{T_0}^{T} -exp\frac{E}{RT}dT \quad (3)$$

where $g(a)$ is the function of conversion ratio a, which is illustrated in **Table 3**. In general, the reaction mechanisms contain chemical reaction (O1, O2, and O3), phase boundary reaction (R1 and R2), and diffusion reaction (D1, D2, D3, and D4) [17].

Table 3 Reaction models and correspondent and g(a) functions

Mechanism and model	g(α)
Chemical reaction order controlled	
First order – O1	$-\ln(1-\alpha)$
Second order – O2	$(1-\alpha)^{-1}$
Third order – O3	$(1-\alpha)^{-2}$
Phase boundary controlled	
Contracting cylinder – R2	$1-(1-\alpha)^{1/2}$
Contracting sphere – R3	$1-(1-\alpha)^{1/3}$
Diffusion controlled	
1D diffusion – D1	α^2
Valensi, 2D – D2	$(1-\alpha)\ln(1-\alpha)+\alpha$
Jander, 3D – D3	$\left[1-(1-\alpha)^{1/3}\right]^2$
Ginstling-Brounshtein, 3D – D4	$1-2\alpha/3-(1-\alpha)^{2/3}$

Coats-Redfern method is extensively applied to calculate the kinetic parameters of coal and biomass during combustion [6]. Therefore, **Eq.3** is integrated, giving:

$$\ln\left[\frac{g(a)}{T^2}\right]=\ln\left[\frac{AR}{wE}\left(1-\frac{2RT}{E}\right)\right]-\frac{E}{RT} \quad (4)$$

Because *2RT/E* is much less than 1 in most combustion reactions, ln[AR/BE*(1-2RT/E)] is always constant in **Eq.4** [9]. Therefore, ln[$g(a)/T^2$] is plotted versus 1/T and a straight line with highest correlation coefficient (R^2) is obtained when g(a) is suitable for the reaction. Then, the corresponding *E, A* values can be calculated.

3. Results and discussion

3.1 The properties of BC, XL and BP

The properties of BC, XL, and BP samples are presented in **Table 2**. It is obvious that the BP has the highest level of volatile content, and the lowest level of ash content.

In addition, the nitrogen (N) and sulfur (S) contents in BP are lower than BC and XL, indicating the characteristic of clean combustion. The properties of BP are similar to those of wood and straw pellets reported in previous studies [20]. In comparison with BC and XL, BP has a higher ratio of volatile to fixed carbon (approximately 4.0), indicating easier ignition. Moreover, the higher oxygen and hydrogen contents are helpful to raise the thermal reactivity. Therefore, the addition of BP in coal can promote the ignition temperature and improve the co-combustion. The fixed carbon concentration of BC is greater than that of XL, so there is a higher calorific value (20.72 kJ/kg) in BC sample. It is also interesting to note that the heating value of BP is higher than that of XL (17.80 kJ/kg >15.68 kJ/kg), which can be explained by the lower carbon content in XL. Previous research has also indicated that lignite form Xiao longtan is kind of coal with lower calorific value [21]. Moreover, the high heating value of BP (17.80 kJ/kg) suggests that it is presumably a better fuel choice.

In addition, it is found that BP contains more alkali metals as compared to coal, which may aggravate slagging problem [22]. High level of alkali metals in XL also indicates that it is a kind of low-grade coal and has some characteristics similar to biomass. Meanwhile, high level of calcium and sulfur are found in XL, explaining the necessity of pollutants control in the process of lignite combustion. In general, the emission of sulfur dioxides can be reduced by adding limestone to coal combustion, as shown in **Eq.5** [23].

$$CaCO_3 = CaO + CO_2; \quad CaO + SO_2 + 0.5O_2 = CaSO_4 \qquad (5)$$

3.2 Thermogravimetric analysis of BC, XL and BP

As shown in **Fig. 1**, there is an obvious difference among thermal behaviors of BC, XL, and BP, while the same moisture dehydration range can be observed at approximately 80-180 °C. The order of weight loss between 80 and 180 °C is: XL>BP>BC, which is consistent with the moisture contents of raw materials in **Table 2**.

For BC, the combustion process is mainly observed between 400 and 700 °C with a maximum weight loss rate 9.0 %/min at about 575 °C, which is caused by the simultaneous combustion of volatile matter and char. It is worth noting that there is a weak second oxidation region from 700 to 800 °C, may representing the decomposition of carbonates, such as calcite and dolomite. The main component of the calcite and dolomite is calcium carbonate, which can be explained by calcium (Ca) in **Table 2**. In addition, previous reports have demonstrated that calcium carbonate undergoes thermal decomposition above 650 °C and the decomposition ends about 800 °C [24, 25], which is consistent with the decomposition temperature in this experiment. Because the calcium content is less in BC, the corresponding oxidation peak is not very obvious. The same conclusion has been confirmed by Hiçyılmaz's TG research on bituminous coal [26].

As for XL, it is decomposed over a broad temperature range without obvious peak, which means the oxidation occurs at a relatively low rate during almost the whole temperature range. XL is a kind of inferior coal, including significant C=O and C-H bonds with low energies, which are easier to decompose than C=C bond in BC [6, 27]. From the above reason, it is found that the ignition temperature and maximum

combustion rate increase with increasing coal quality from XL to BC. This is consistent with previous conclusions [26, 28]. Similarly, second peak at 750 °C attributed to carbonates is found from the thermodynamic curves. XL contains more calcium (32.62 g/kg) than BC (12.12 g/kg) in **Table 2**. Thus the mass loss of XL during the second oxidation region is greater than that of BC in **Fig.1** (7.5% > 2.08%).

Different from BC and XL, the combustion of BP is clearly divided into two stages: the release and burn of volatile matter (250-400 °C), and the combustion of fixed carbon (400-550°C). As a kind of biomass, cellulose and hemicellulose are major chemical constituents, and their decomposition temperature ranges are from 220 to 315 °C and from 315 to 400 °C, respectively [29]. Therefore, the first combustion stage of BP is mainly attributed to the decomposition and combustion of hemicellulose and cellulose, and the mass loss accounts for about 62.59%. Lignin has high stability and decomposes over a broad temperature (160-627 °C) [30]. Therefore, fixed carbon and some lignin decompose at the second stage. It is clear that BP decomposes much faster than coal at the same temperature. Previous conclusions [31, 32] have indicated that the polymers of cellulose, hemicelluloses and lignin are linked by relatively weak bonds (380–420 kJ/mole energy), which are easy to be broken down.

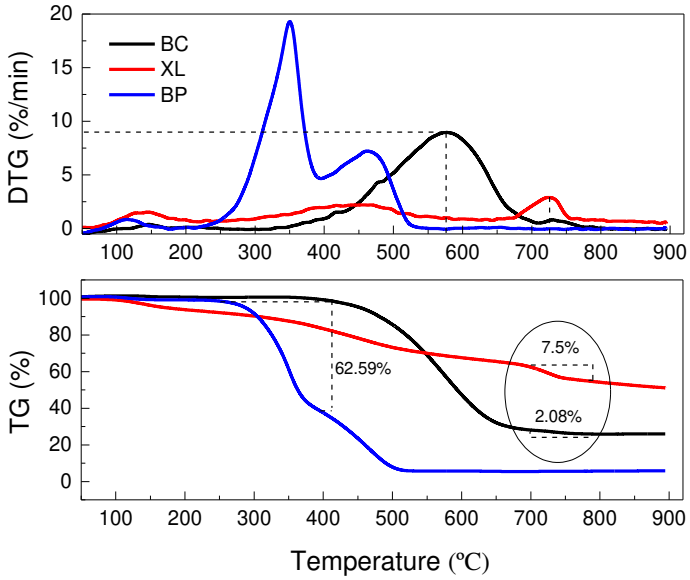

Fig. 1. DTG and TG curves for BC, XL and BP

3.3 Co-combustion of BC, XL and BP

Fig. 2 presents DTG curves of different blends arranged in order according to the mass proportion of BP. Dehydration and decomposition of carbonates are not discussed in this paper.

For blends of BC and BP, they display three step mass losses (stages 1, 2 and 3). Stages 1 and 2 are mainly belonged to the release and combustion of volatile matter, and the char oxidation of BP, respectively. Stage 3 is mostly attributed to the combustion of BC. With the increasing BP proportion, the peak combustion rate increases continuously at stages 1 and 2, and decreases gradually at stage 3, due to the elevated volatile matter, BP-char and reduced BC-char, respectively. Moreover, the second peak of BP (stage 2) and the peak of the coal (stage 3) overlap together as the mass ratio of BP is less than 50%. The same overlap between coal and biomass has been found in previous research [17]. In addition, remaining mass of residual sample is also decreasing, suggesting the combustion of BC is promoted due to the addition of

BP. For blends of XL and BP, only two obvious burning stages are observed in DTG profiles. The curve of stage 1 is mainly due to the release and combustion of volatile matter in BP and XL, while stage 2 is the combustion of BP-char and XL. Similarly, peak burning rate of the first evolution profile increases with increasing BP ratio. However, DTG profile in stage 2 displays an irregular variation with the addition of BP. It is assumed that there is no interaction between BP and XL. Because the burning rate of BP is far greater than that of XL, the DTG profile in stage 2 should show a regular variation, which depends on the BP ratio in the blends. However, experimental results are the opposite, suggesting that there is an interaction between BP and XL, which is discussed further in the next section.

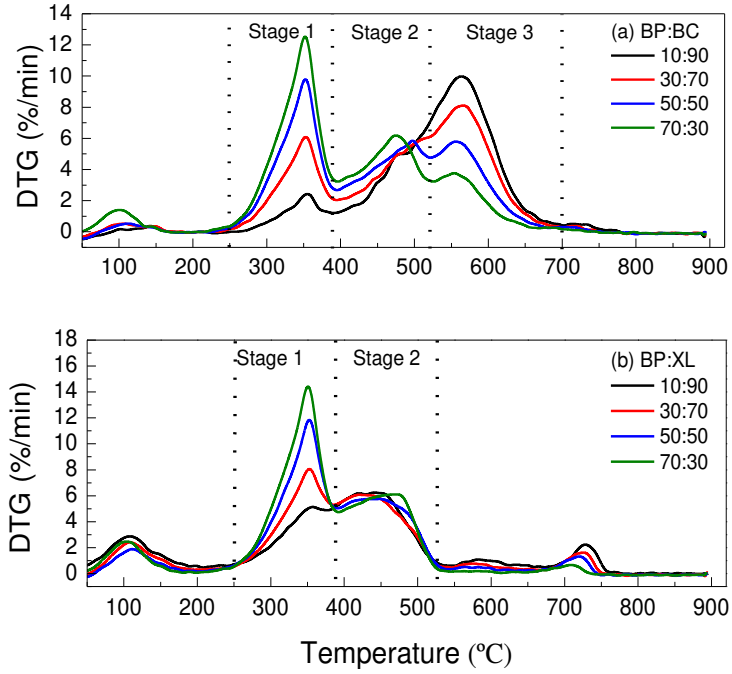

Fig. 2. DTG curves for the co-combustion of (a) BC and BP and (b) XL and BP

The combustion characteristic parameters are presented in **Table 4**. In order to investigate the influence of BP addition on coal (BC and XL) combustion, **Fig. 3** is established. For all blends, it is found that T_i and T_b decrease with increasing BP

proportion, indicating combustion process is shifting forward by adding BP. In addition, DTG_a and *S* increase with increasing BP ratio in blends due to the higher volatile matter than coal. Thus it is expected that the blending of BP with BC or XL would promote the combustion property. Similar thermal characteristics due to the presence of biomass are also reported by previous studies [8, 33, 34].

The maximum burning rates corresponding to different combustion stages are DTG_1, DTG_2, and DTG_3, respectively. **Fig. 3 (c)** presents that DTG_1 for all blends almost increases linearly with increasing BP proportion. A greater number of volatiles are formed and ignited due to the presence of BP in the blends. This result suggests that the higher BP ratio, the faster mass loss rate, in other words, the higher blends reactivity in stage 1. It is confirmed that the maximum burning rate is positively related to thermal reactivity [35, 36]. Nevertheless, DTG_3-BC for the BC/BP blends is generally reduced with elevated BP ratio, which may result in negative effect on thermal reactivity. Accordingly, a desirable percentage of BP should be selected for co-combustion of BC and BP. Unlike BC/BP, DTG_2-XL for XL/BP has a significant rise due to the added BP, and then the overall variation tends to be stable. This phenomenon seems to show that the more BP, the more conducive to the combustion of XL/BP. However, XL contains more ash and more alkaline metals than BC, and it is more likely to be slagging during combustion with biomass. Thus, it is still important to choose the appropriate BP proportion during the co-combustion of XL and BP.

Table 4 Characteristic parameters for all samples

Samples	T_i	T_b	Stage 1	Stage 2	Stage 3	DTG_a	*S*

		(°C)	(°C)	T_1 (°C)	DTG_1 (%/min)	T_2 (°C)	DTG_2 (%/min)	T_3 (°C)	DTG_3 (%/min)	(%/min)	(10^{-7})
BC:BP	100:0	490	800	/	/	/	/	577	8.96	1.68	0.78
	90:10	470	775	355	2.43	/	/	565	9.97	1.70	0.99
	70:30	440	748	353	6.08	/	/	565	8.10	1.84	1.32
	50:50	319	743	352	9.78	497	5.84	558	5.80	1.86	2.56
	30:70	315	710	352	12.53	474	6.18	555	3.95	1.95	3.47
	0:100	318	550	350	19.28	466	7.22	/	/	2.14	7.42
XL:BP	100:0	345	900	/	/	455	2.21	/	/	1.61	0.33
	90:10	335	775	356	5.13	441	6.24	/	/	1.68	1.23
	70:30	320	750	352	8.05	430	6.07	/	/	1.72	1.76
	50:50	320	745	352	11.83	448	5.75	/	/	1.79	2.78
	30:70	318	730	351	14.4	471	6.10	/	/	1.94	3.78
	0:100	318	550	350	19.28	466	7.22	/	/	2.14	7.42

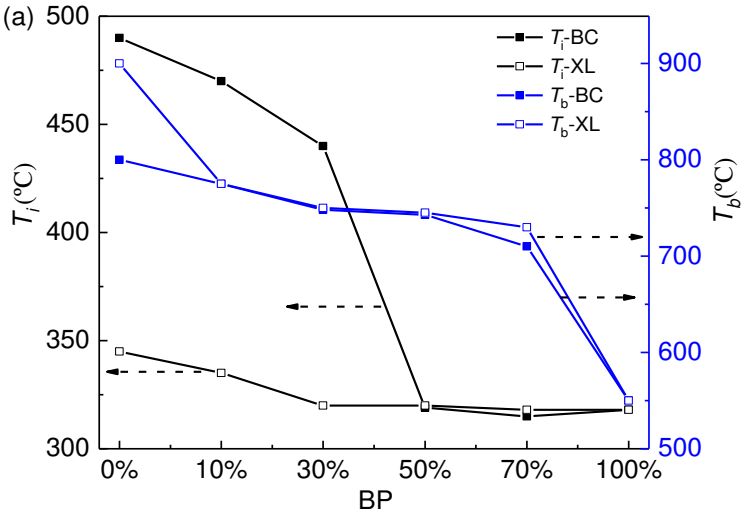
(a)
T_i-BC
T_i-XL
T_b-BC
T_b-XL
T_i(℃)
T_b(℃)
BP
0%
10%
30%
50%
70%
100%

287

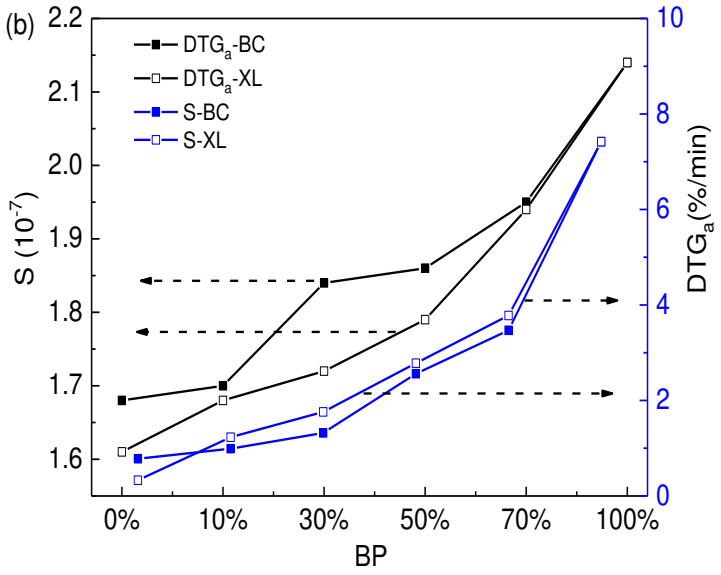
(b)
DTG$_a$-BC
DTG$_a$-XL
S-BC
S-XL
S (10^{-7})
DTG$_a$(%/min)
BP
0%
10%
30%
50%
70%
100%

288

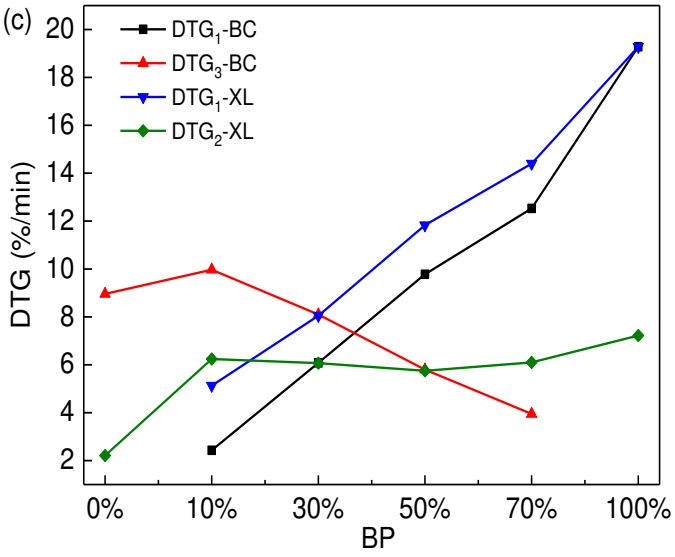
(c)
DTG$_1$-BC
DTG$_3$-BC
DTG$_1$-XL
DTG$_2$-XL
DTG (%/min)
BP
0%
10%
30%
50%
70%
100%

289

290 **Fig. 3.** Relationship between combustion characteristic parameters and BP percentage: (a) T_i , T_b;

291 (b) DTG_a, S; (c) DTG_1, DTG_2, DTG_3

292 **3.4. Interaction between BC, XL and BP**

293 In order to investigate interaction between coal and biomass, theoretical

294 thermodynamic behavior of the blends are obtained using the following formula [37].

295 $$TG = X_c * TG_c + X_b * TG_b \quad (6)$$

296 where TG_c and TG_b represent the weight loss of coal and biomass, respectively. X_c and

297 X_b are the percentages of coal and biomass, respectively. The theoretical TG curves at

298 different percentages of BP (10%, 30%, 50% and 70%) are calculated. All the

299 experimental and calculated TG curves are presented in **Fig. 4**. Moreover, deviations

300 (subtract calculated TG from experimental TG) representing possible interaction

301 between coal and biomass are also depicted.

302 The results show that TG curves for BC/BP blends are very similar, especially

303 when the temperature is below 500 ºC. Some clear differences are visible above this

304 temperature and disappear gradually as temperature is above 700 ºC. Although similar

305 differences have been found in previous research by Zhou et al. [36], it was considered

306 that this is an experimental deviation and there was no interaction. However, repeatable

307 test in our experiment shows that this kind of difference always exists. Moreover, the

308 maximum deviation is large enough (-7.69% for blends with 30% BP). Yao et al. found

309 the interaction in co-fuels by the largest TG deviation 7.41% at 323 ºC [38]. Based on

310 the above analyses, there should be an interaction between BC and BP. But this

311 synergistic effect is relatively weak and mainly concentrated in stage 3 (500-700 ºC)

312 due to BC combustion. The specific mechanisms involved in different coal with
313 biomass require further investigation. In addition, it is found that synergistic interaction
314 is not proportional to BP ratio, which is consistent with previous research [13]. Li et al.
315 found that interaction between distillation residue and lignite was decreased as the
316 distillation residue ratio is higher than 60%, due to the poor contact [13]. In our paper,
317 the order of deviation of BC/BP with different BP proportion is: 30%>10%>50%>70%.

318 Unlike BC/BP blends, there are very obvious deviations in XL/BP when
319 temperature is above 300 ºC, and the difference reaches the maximum value -29.86%
320 at 500 ºC. This temperature range (300-500 ºC) is the main combustion zone of XL/BP
321 displayed in **Fig. 2(b)**. Compared with BC/BP (500-700 ºC, -7.69%), the interaction of
322 XL and BP begins early and is more obvious. This is mainly due to the distinct
323 combustion characteristics **(Table 4)**, caused by the different chemical compositions
324 and energy bonds of BP and XL. Moreover, it is found that different deviation curves
325 for all blends have almost the same trends as temperature continues to increase, which
326 means deviations decrease gradually with the gradual burnout. In addition, the least BP
327 ratio in XL/BP blends seems to have the greatest deviation, and the order of deviation
328 with different BP ratio is: 10%>30%>50%>70%.

329 The synergistic mechanism between coal and biomass during co-combustion is not
330 very clear. In comparison with calculated results, experimental curves basically shift to
331 low temperature at the same TG. The deviation values are negative except for partial
332 temperature range in BC/BP blends. The reason for negative deviation could be due to
333 the fact that addition of biomass could release more heat, promoting endothermic

reactions, which is favorable for coal burning. Previous researchers report that char generated in the process of biomass decomposition plays a catalytic role for coal degradation, which promotes coal burn completely in advance [32, 39]. In addition, some other reports indicate that the interaction between coal and biomass is mainly controlled by thermal effect [40, 41]. The released heat due to biomass combustion is quickly transferred to coal, enhancing the reaction rate of coal. Some slight positive values in BC/BP (50% and 70% BP) may be caused by experimental errors and ash slagging. Although repeated tests have been carried out, some small deviations (<5%) cannot be completely eliminated. It was reported that coal/biomass co-firing could result in significant changes in ash properties as biomass ratio is greater than 50%. Alkaline/alkaline-earth metals (in biomass) can react with minerals (in coal), which resulted in slagging and agglomeration, decreasing the combustion reactivity [42, 43].

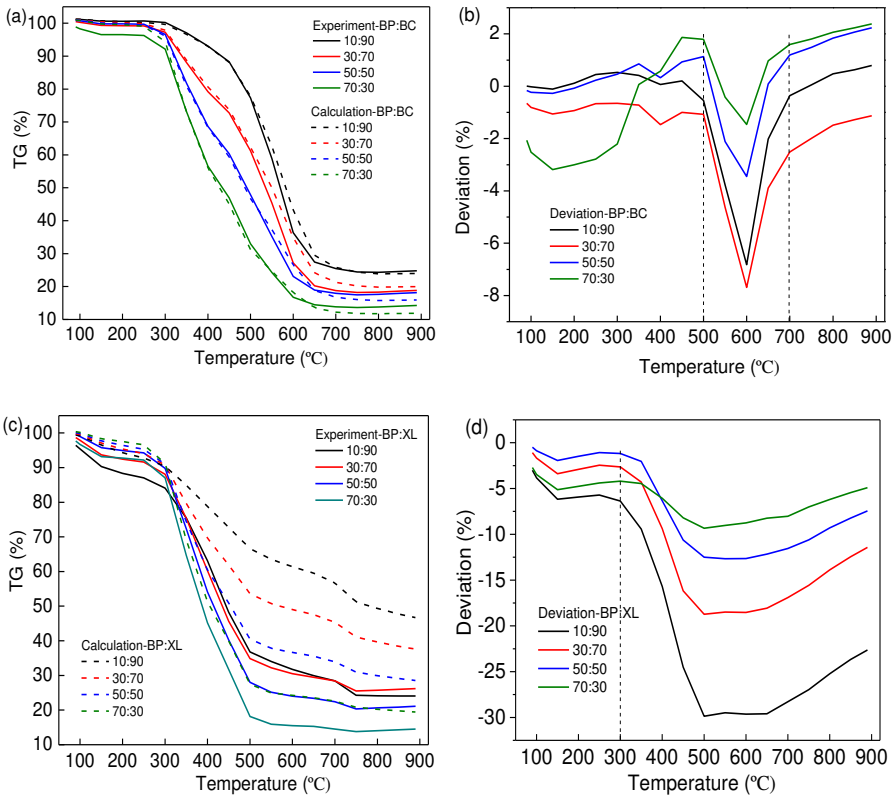

Fig. 4. Experimental, calculated TG curves and their deviations: (a) BC/ BP; (b) deviation of BP/BC; (c) XL/ BP; (d) deviation of XL/BP

3.5. Kinetics

According to the DTG analysis in **Section 3.3**, coal (BC, XL) burning is mainly concentrated in one stage, whereas the combustion of biomass (BP) or coal/biomass blends can be divided into 2 or 3 stages. Therefore, each stage should be analyzed separately, using the most suitable g(a) with highest correlation coefficient. **Figs.S1** and **S2** are the plots of $\ln[g(a)/T^2]$ against 1/T with all reaction models. **Table 5** displays the kinetic parameters with highest correlation coefficient for all samples.

For BC, BP, and BC/BP blends, the chemical first order reaction (O1) correlates best (R^2: 0.9439-0.9941) in stages 1 and 3, suggesting the rate-controlling step is the chemical reaction. Diffusion mechanism (D1) is the most effective for stage 2 during combustion (BP ratio: 50%, 70%, and 100%). These are consistent with the research of Gil et al [17]., who found that O1 model was the most effective mechanism for the first step of biomass oxidation and coal combustion, and D3 was responsible for the second step of biomass combustion. Moreover, the E values (40.92-118.49 kJ/mol) of BC/BP combustion are lower or higher than some previous reported from coal/biomass (141.0-195.5 kJ/mol, 9.1-47.7 kJ/mol) [6, 16]. This may be caused by different sample properties, calculation models and heating rates [17]. In addition, with elevated biomass ratio, the activation energy of blends in first stage is decreasing first and then increasing. Unlike values in stage 1, E presents a downward trend in stage 3, which is similar with Zhou et al.'s research [36]. This indicates that there is an optimal biomass ratio based

on the principle of minimum activation energy. When BP content is 30%, the activation energy is smallest, which is at the same biomass proportion when the deviation is highest from the aforementioned thermogravimetric analysis.

Different from BC/BP blends, D3 mechanism for the first stage and D4 for the second stage have their highest correlation coefficients, respectively (D3:0.9615-0.9883, D4: 0.9830-0.9975). This indicates that the combustion reaction is controlled by diffusion of the oxidizer into the reacting particle. In addition, it is worth nothing that adding biomass can increase activation energy of stage 1, whereas reduce the *E* value in stage 2. This is also consistent with Zhou et al.'s research [36], but not consistent with the trends of combustion properties of blends. Toptas et al. thought that calculated activation energies are not always consistent with the trends of combustion properties of biomasses, depending on biomass type [16]. Additive proportion of 10% BP is recommended for the combustion of BP and BC, due to the minimum activation energy. This conclusion is also consistent with the aforementioned thermogravimetric analysis.

Although an appropriate biomass proportion can be determined based on the minimum activation energy principle, the combustion process involves many aspects, such as gaseous pollutants, heavy metals, ash slagging, etc. In order to choose the optimal proportion of biomass combustion, these studies still need to be completed in future.

Table 5 Kinetic parameters of all samples

Sample	Stage 1	Stage 2	Stage 3

	E	Model	R^2	*E*	Model	R^2	*E*	Model	R^2
100BC							87.95	O1	0.9909
90BC:10BP	118.49	O1	0.9552				61.21	O1	0.9797
70BC:30BP	76.36	O1	0.9941				44.38	O1	0.9439
50BC:50BP	99.87	O1	0.9911	37.17	D1	0.9823	40.92	O1	0.9755
30BC:70BP	87.31	O1	0.9718	32.61	D1	0.9839	43.98	O1	0.9926
100BP	81.62	O1	0.9853	37.45	D1	0.9926			
100XL				51.90	D4	0.9927			
90XL:10BP	47.07	D3	0.9766	48.67	D4	0.9830			
70XL:30BP	81.81	D3	0.9883	46.45	D4	0.9876			
50XL:50BP	95.46	D3	0.9673	43.34	D4	0.9975			
30XL:70BP	95.32	D3	0.9615	41.80	D4	0.9930			

4. Conclusions

Co-combustion of BP and the two kinds of coal (BC and XL) is investigated using a thermogravimetric analyzer. The combustion process of BP and BC is divided into three stages, including the release and combustion of volatile matter, oxidation of BP char, and the combustion of BC char. However, there are only two stages for XL/BP blends, which are the combustion of volatile matter in BP and XL, and the char burning of BP and XL. With increasing BP ratio, the maximum combustion rate and combustion index increase, while the burnout temperature decreases, indicating the combustion performance of coal can be improved.

Due to different properties of coal, interactions between BP and XL are more obvious than that of BP and BC. The maximum deviations are 30% BP for BC/BP and

10% BP for XL/BP, respectively. Kinetic analysis indicates that the O1 model is the reaction mechanism of biomass burn in first stage and coal combustion in BC/BP blends. D3 and D4 mechanisms are suitable for the second stage of biomass burn and XL combustion, respectively. Moreover, the minimum activation energies of biomass blending ratio are 30% for BC/BP and 10% for XL/BP.

AUTHOR INFORMATION

Corresponding Author

E-mail: zzhong@seu.edu.cn; A.Hassanpour@leeds.ac.uk

Notes

The author declares no competing financial interest.

ACKNOWLEDGEMENTS

The authors are grateful to the support given by the National Natural Science Fund Programs of China (51776042, U1361115), Scientific Research Foundation of Graduate School of Southeast University (YBJJ1644), Newton Foundation and China Scholarship Council.

REFERENCES

[1] A. Cancela, A. Sanchez, X. Alvarez, A. Jimenez, L. Ortiz, E. Valero, P. Varela, Pellets valorization of waste biomass harvested by coagulation of freshwater algae, Bioresource Technol 204 (2016) 152-156.

[2] T. Zeng, A. Pollex, N. Weller, V. Lenz, M. Nelles, Blended biomass pellets as fuel for small scale combustion appliances: Effect of blending on slag formation in the bottom ash and pre-evaluation options, Fuel 212 (2018) 108-116.

[3] F.H. Guo, Z.P. Zhong, Experimental studies on combustion of composite biomass pellets in fluidized bed, Sci Total Environ 599 (2017) 926-933.

[4] Q. Li, J.K. Jiang, S.Y. Cai, W. Zhou, S.X. Wang, L. Duan, J.M. Hao, Gaseous Ammonia Emissions from Coal and Biomass Combustion in Household Stoves with

Different Combustion Efficiencies, Environ Sci Tech Let 3(3) (2016) 98-103.
[5] S.S. Idris, N.A. Rahman, K. Ismail, Combustion characteristics of Malaysian oil palm biomass, sub-bituminous coal and their respective blends via thermogravimetric analysis (TGA), Bioresource Technol 123 (2012) 581-591.
[6] D. Magalhaes, F. Kazanc, J. Riaza, S. Erensoy, O. Kabakli, H. Chalmers, Combustion of Turkish lignites and olive residue: Experiments and kinetic modelling, Fuel 203 (2017) 868-876.
[7] R. Junga, W. Knauer, P. Niemiec, M. Tanczuk, Experimental tests of co-combustion of laying hens manure with coal by using thermogravimetric analysis, Renew Energ 111 (2017) 245-255.
[8] K. Jayaraman, M.V. Kok, I. Gokalp, Thermogravimetric and mass spectrometric (TG-MS) analysis and kinetics of coal-biomass blends, Renew Energ 101 (2017) 293-300.
[9] J. Wang, S.Y. Zhang, X. Guo, A.X. Dong, C. Chen, S.W. Xiong, Y.T. Fang, W.D. Yin, Thermal Behaviors and Kinetics of Pingshuo Coal/Biomass Blends during Copyrolysis and Cocombustion, Energ Fuel 26(12) (2012) 7120-7126.
[10] H. Ullah, G.J. Liu, B. Yousaf, M.U. Ali, Q. Abbas, C.C. Zhou, Combustion characteristics and retention-emission of selenium during co-firing of torrefied biomass and its blends with high ash coal, Bioresource Technol 245 (2017) 73-80.
[11] G.W. Wang, J.L. Zhang, J.G. Shao, Z.J. Liu, G.H. Zhang, T. Xu, J. Guo, H.Y. Wang, R.S. Xu, H. Lin, Thermal behavior and kinetic analysis of co-combustion of waste biomass/low rank coal blends, Energ Convers Manage 124 (2016) 414-426.
[12] Z.G. Liu, A. Quek, S.K. Hoekman, M.P. Srinivasan, R. Balasubramanian, Thermogravimetric investigation of hydrochar-lignite co-combustion, Bioresource Technol 123 (2012) 646-652.
[13] H. Li, S.Q. Xia, P.S. Ma, Thermogravimetric investigation of the co-combustion between the pyrolysis oil distillation residue and lignite, Bioresource Technol 218 (2016) 615-622.
[14] D. Yu, M.Q. Chen, Y.H. Wei, S.B. Niu, F. Xue, An assessment on co-combustion characteristics of Chinese lignite and eucalyptus bark with TG-MS technique, Powder Technol 294 (2016) 463-471.
[15] D. Vamvuka, S. Sfakiotakis, Combustion behaviour of biomass fuels and their blends with lignite, Thermochim Acta 526(1-2) (2011) 192-199.
[16] A. Toptas, Y. Yildirim, G. Duman, J. Yanik, Combustion behavior of different kinds of torrefied biomass and their blends with lignite, Bioresource Technol 177 (2015) 328-336.
[17] M.V. Gil, D. Casal, C. Pevida, J.J. Pis, F. Rubiera, Thermal behaviour and kinetics of coal/biomass blends during co-combustion, Bioresource Technol 101(14) (2010) 5601-5608.
[18] K. Kirtania, S. Bhattacharya, Pyrolysis kinetics and reactivity of algae-coal blends, Biomass Bioenerg 55 (2013) 291-298.
[19] H.Y. Meng, S.Z. Wang, L. Chen, Z.Q. Wu, J. Zhao, Investigation on Synergistic Effects and Char Morphology during Co-pyrolysis of Poly(vinyl chloride) Blended with Different Rank Coals from Northern China, Energ Fuel 29(10) (2015) 6645-

6655.
[20] R. Chirone, P. Salatino, F. Scala, R. Solimene, M. Urciuolo, Fluidized bed combustion of pelletized biomass and waste-derived fuels, Combust Flame 155(1-2) (2008) 21-36.
[21] Z.H. Guo, Q.H. Wang, M.X. Fang, Z.Y. Luo, K.F. Cen, Thermodynamic and economic analysis of polygeneration system integrating atmospheric pressure coal pyrolysis technology with circulating fluidized bed power plant, Appl Energ 113 (2014) 1301-1314.
[22] D.Y. Wu, Y.H. Wang, Y. Wang, S. Li, X.L. Wei, Release of alkali metals during co-firing biomass and coal, Renew Energ 96 (2016) 91-97.
[23] S.L. Niu, K.H. Han, C.M. Lu, Release of sulfur dioxide and nitric oxide and characteristic of coal combustion under the effect of calcium based organic compounds, Chem Eng J 168(1) (2011) 255-261.
[24] J.P. Sanders, P.K. Gallagher, Kinetic analyses using simultaneous TG/DSC measurements Part I: decomposition of calcium carbonate in argon, Thermochim Acta 388(1-2) (2002) 115-128.
[25] F.S. Murakami, P.O. Rodrigues, C.M.T. de Campos, M.A.S. Silva, Physicochemical study of CaCO3 from egg shells, Ciencia Tecnol Alime 27(3) (2007) 658-662.
[26] C.Hiçyılmaz, Comparison of the Combustion Characteristics of Three Different Fossil Fuels from Turkey 1St^{h} International Mining Congress and Exhibition of Turkey-IMCET 2003 (2003) 401-406.
[27] T.Q. To, K. Shah, P. Tremain, B.A. Simmons, B. Moghtaderi, R. Atkin, Treatment of lignite and thermal coal with low cost amino acid based ionic liquid-water mixtures, Fuel 202 (2017) 296-306.
[28] W.Q. Zhang, S.G. Jiang, K. Wang, L.Y. Wang, Y.L. Xu, Z.Y. Wu, H. Shao, Y.H. Wang, M.L. Miao, Thermogravimetric Dynamics and FTIR Analysis on Oxidation Properties of Low-Rank Coal at Low and Moderate Temperatures (vol 35, pg 39, 2015), Int J Coal Prep Util 35(2) (2015) 111-111.
[29] L. Aguiar, F. Marquez-Montesinos, A. Gonzalo, J.L. Sanchez, J. Arauzo, Influence of temperature and particle size on the fixed bed pyrolysis of orange peel residues, J Anal Appl Pyrol 83(1) (2008) 124-130.
[30] A. Ounas, A. Aboulkas, K. El Harfi, A. Bacaoui, A. Yaacoubi, Pyrolysis of olive residue and sugar cane bagasse: Non-isothermal thermogravimetric kinetic analysis, Bioresource Technol 102(24) (2011) 11234-11238.
[31] M. Yilgin, N.D. Duranay, D. Pehlivan, Co-pyrolysis of lignite and sugar beet pulp, Energ Convers Manage 51(5) (2010) 1060-1064.
[32] Z.Q. Xie, X.Q. Ma, The thermal behaviour of the co-combustion between paper sludge and rice straw, Bioresource Technol 146 (2013) 611-618.
[33] M. Otero, M.E. Sanchez, X. Gomez, Co-firing of coal and manure biomass: A TG-MS approach, Bioresource Technol 102(17) (2011) 8304-8309.
[34] M.L. Contreras, F.J. Garcia-Frutos, A. Bahillo, Study of the thermal behaviour of coal/biomass blends during oxy-fuel combustion by thermogravimetric analysis, J Therm Anal Calorim 123(2) (2016) 1643-1655.

[35] D. Vamvuka, E. Kakaras, E. Kastanaki, P. Grammelis, Pyrolysis characteristics and kinetics of biomass residuals mixtures with lignite, Fuel 82(15-17) (2003) 1949-1960.
[36] C.C. Zhou, G.J. Liu, T. Fang, P.K.S. Lam, Investigation on thermal and trace element characteristics during co-combustion biomass with coal gangue, Bioresource Technol 175 (2015) 454-462.
[37] K.M. Lu, W.J. Lee, W.H. Chen, T.C. Lin, Thermogravimetric analysis and kinetics of co-pyrolysis of raw/torrefied wood and coal blends, Appl Energ 105 (2013) 57-65.
[38] Z.L. Yao, X.Q. Ma, Z.H. Wang, L.M. Chen, Characteristics of co-combustion and kinetic study on hydrochar with oil shale: A thermogravimetric analysis, Appl Therm Eng 110 (2017) 1420-1427.
[39] Y.F. Liao, X.Q. Ma, Thermogravimetric analysis of the co-combustion of coal and paper mill sludge, Appl Energ 87(11) (2010) 3526-3532.
[40] Y.Y. Zhang, Z.Z. Zhang, M.M. Zhu, F.Q. Cheng, D.K. Zhang, Interactions of coal gangue and pine sawdust during combustion of their blends studied using differential thermogravimetric analysis, Bioresource Technol 214 (2016) 396-403.
[41] X.Y. Huang, X.M. Jiang, X.X. Han, H. Wang, Combustion Characteristics of Fine- and Micro-pulverized Coal in the Mixture of O-2/CO2, Energ Fuel 22(6) (2008) 3756-3762.
[42] S.F. Miller, H.H. Schobert, Effect of the Occurrence and Modes of Incorporation of Alkalis, Alkaline-Earth Elements, and Sulfur on Ash Formation in Pilot-Scale Combustion of Beulah Pulverized Coal and Coal-Water Slurry Fuel, Energ Fuel 8(6) (1994) 1208-1216.
[43] D.E. Priyanto, S. Ueno, N. Sato, H. Kasai, T. Tanoue, H. Fukushima, Ash transformation by co-firing of coal with high ratios of woody biomass and effect on slagging propensity, Fuel 174 (2016) 172-179.